PCCP

Accepted Manuscript

ROYAL SOCIETY OF CHEMISTRY

www.rsc.org/pccp

PCCP

RSCPublishing

ARTICLE

Colorimetric and fluorimetric response of Schiff base molecules towards fluoride anion, solution test kit fabrication, logical interpretations and DFT-D3 study

Cite this: DOI: 10.1039/x0xx00000x

Received 00th January 2012,
Accepted 00th January 2012

DOI: 10.1039/x0xx00000x

www.rsc.org/

Pritam Ghosh,[a] Biswajit Gopal Roy,[c] Saibal Jana,[d] Subhra Kanti Mukhopadhyay[e] and Priyabrata Banerjee*[ab]

Two newly synthesized Schiff base molecules are hereby reported as anion sensor. -NO_2 substituted comparatively higher acidic receptor (P1) can sense F^-, OAc^- and $H_2PO_4^-$, whereas -CN substituted less acidic receptor (P2) is selective for F^- only. Reversible UV-Vis response for both receptors with F^- can mimic multiple logic gate function and eventually several complex electronic circuit based on XNOR, XOR, OR, AND, NOT and NOR logic operations with '*Write-Read-Erase-Read*' option have been executed. Interesting fluorescence '*turn on* and *off*' responses are noticed for the receptors with F^-. Intracellular F^- detection as a diagnosis of non skeletal fluorosis is successful using fluorescence microscope in *Candida albicans* (prokaryotic cell, a diploid fungus) and pollen grains of *Techoma stans* (eukaryotic cell), incubated in 10^{-6}M fluoride contaminated hand pump water collected from Bankura, West Bengal, India. Furthermore, one solution test kit is fabricated for easy and selective detection of F^- in aqueous solvent.

Introduction

In recent year's biologically essential anion detection is an emergent area of interest for the researchers. The awareness of scientific society in this field is triggered by the growing requirement of sensitive and selective sensors development for anion detection as anions are known to be indispensible concerning their long range impact on biological, chemical and environmental related issues.[1] In literature, their utility and usefulness are also well documented.[1] In this context, till date several anion sensors have been reported by scientific community.[2] In general most of the reported and common sensor design involves polarization of -NH protons of urea or thiourea,[2] pyrrole,[2] amide[2] and imidazolium[2] moieties where design strategies are mostly sophisticated, expensive and sometimes delayed response are also coming for a particular recognition event.[2] In view of above designed synthesis of several Schiff bases have been studied as anion sensors because these are easy to prepare and can be modified according to choice.

As a part of our ongoing research on supramolecular chemistry[3] our aim is to find out simple synthesis route, convenient operation path and very selective and specific chemosensor especially for fluoride anion. Inspite of playing a vital role in dental care and clinical osteoporosis[3b,3e,4] fluorides adverse effects are also documented by researchers worldwide. Excess of this anion's presence can result in gastric and kidney disorders urolithiasis, dental and skeletal flurosis.[3b,5] The third world is at risk many a times due to flooding, which may enhance fluoride concentration in drinking water. Side by side, fluoride is also known as a hydrolyzed product of organophosphorus chemical weapons.[6a] Therefore selective detection of biologically and chemically important anions like fluoride is of foremost significance. Particular interest in this regard is colorimetric sensing which would allow naked eye detection by an easy and straight forward way.[6b] It is always preferable to have potential hydrogen bond donor like -OH, -NH groups in chemo sensor which in turn can increase the attraction of sensor towards F^- *via* highly dissociable protons. In general sensor (host) having -OH, -NH group, shows better responses in terms of host-guest interaction for guest F^-. The acidic protons may be abstracted by anion like F^- where charge *vs* radius ratio is very high. The sensor acts as a brönsted acid while the anion is as brönsted base. This type of molecular scaffolds with enhanced acidity commonly suffers from multi anion interference with the oxo anions like OAc^-, $H_2PO_4^-$ with inherent structural bulkiness and comparatively less charge *vs* radius ratio than that of F^-. Therefore to make a sensor more selective towards fluoride recognition, it is perhaps necessary to minimize the chelating capability of sensor, which can be done by selective removal of the -OH group from the sensor of interest. Another important issue and perhaps the key factor in this regard is the suitable substitution effect on sensors aromatic ring. -NO_2 group as chromophore are used for generation of chromogenic sensor and which exerts both –R and –I effects. In its consequence acidity of the -NH proton are increased. However, use of other substitution like cyanide (-CN) may also influence the -NH proton differently and as a consequence the acidity can be controlled in order to make less acidic but highly selective sensor.

We hereby demonstrate two anion sensors: 2-(4-bromobenzylidene)-1-(2,4-dinitrophenyl)hydrazine namely **P1** and 4-(2-(4-bromobenzylidene)hydrazinyl)benzonitrile as **P2**. Between these two anion sensors, **P2** can sense fluoride selectively among other anions present like Cl^-, Br^-, I^-, OAc^-, SO_4^{2-}, $C_2O_4^{2-}$, SCN^-, $H_2PO_4^-$, HPO_4^{2-}, HSO_4^-, ClO_4^-, PF_6^-, BF_4^-, N_3^-, NO_2^-, NO_3^-, CO_3^{2-} and **P1** can sense F^-, OAc^- and $H_2PO_4^-$ from rest of the anions. To our belief, perhaps this report also demonstrate a clear picture about how the effect of substitution on an aromatic sensor ring makes **P1** more acidic and build it responsible for multi anion sensing while for **P2,** tunes it more selective only towards F^- anion. As our main focus is to

develop a selective fluoride sensor, therefore we will discuss on sensor···F^- interaction chemistry from the angle of experimental outcome as well as from theoretical perspective. In experimental investigation both **P1** and **P2** sensors are examined through UV-Vis, fluorescence and ^{1}H-NMR titration with TBA salt of F^-. HF_2^- formation is not only validated as a proof of acid-base reaction between host (**P1**) and guest (F^-) by experiments but also fully supported by modern Density Functional Theory (DFT-D3) calculation. The interesting spectral responses of sensor **P1** and **P2** towards an external stimulus like F^- inspired us to design circuit for electronic devices (*i.e.;* molecular logic gates here). In recent days, molecules with appreciable number of reversibility cycles in their spectral responses towards an external stimulus have gained appreciable importance for development of new electronic devices in information technology. As a basis of current computers, electronic logic gates perform binary arithmetic and several different logical operations. Logic gates are mainly typical switches with input (0 or 1) and output mode (0 or 1).[7] In this present work, we have described herein the possibility of developing simple to complex circuit with single or dual output mode. Combinations of different circuits based on principles of AND-NOT-OR-XOR-NOR-XNOR logic gates are designed. Nevertheless, solution test kit development for selective detection of anions with proper discrimination between F^- and OAc^- or $H_2PO_4^-$ from unidentified sample in aqueous solvent mixture [DMSO:Water (4:1)] has been developed to make the sensors more applicable in real life. The Bio-medical relevance of sensor **P1** is also explored by detecting intracellular F^- from pollen grains of *Techoma stans* (eukaryotic cell) and *Candida albicans* (prokaryotic cell, a diploid fungus).

Results and Discussion

P1 and **P2** were synthesized by an easy Schiff base condensation technique (see ESI†, Section 1, Scheme S1 and S2). Formation was confirmed by ESI-MS, ^{1}H-NMR like sophisticated analytical tools (see ESI† for details, Fig. S1-S4, crystallographic details were tabulated in Table S1-S3). The geometry optimized structure of **P1** was shown in Fig. 1a and ORTEP of **P2** is shown in Fig. 1b.

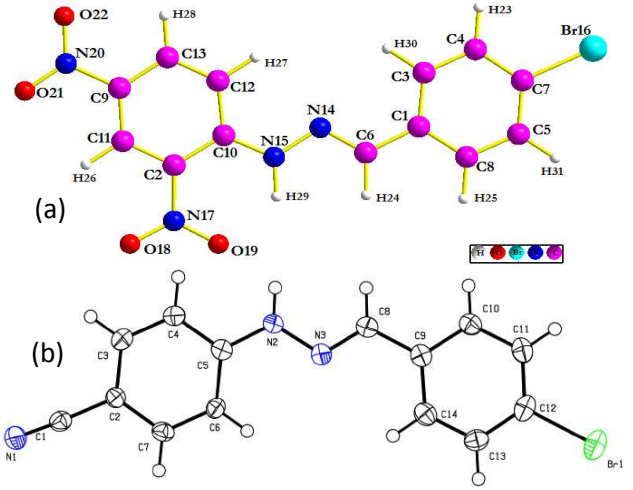

Fig. 1 (a) Optimized structure of **P1** and (b) ORTEP of **P2**.

Visual Colorimetric responses of P1 and P2 with anions

Visual color changes of **P1** and **P2** ($1.0x10^{-4}$M) in DMSO at room temperature is investigated. Intense and sharp color changes instantly from yellow to red for **P1** with F^-, OAc^- and $H_2PO_4^-$ (Fig. 2a) and from colourless to bright yellow in presence of only F^- is noticed for **P2** (Fig. 2b). It is noteworthy, upon addition of TBA salts of other anions there is no detectable response for **P2**. **P1** also remains silent for other competing anions like Cl^-, Br^-, I^-, SO_4^{2-}, $C_2O_4^{2-}$, SCN^-, HPO_4^{2-}, HSO_4^-, ClO_4^-, PF_6^-, BF_4^-, N_3^-, NO_2^-, NO_3^- and CO_3^{2-}.

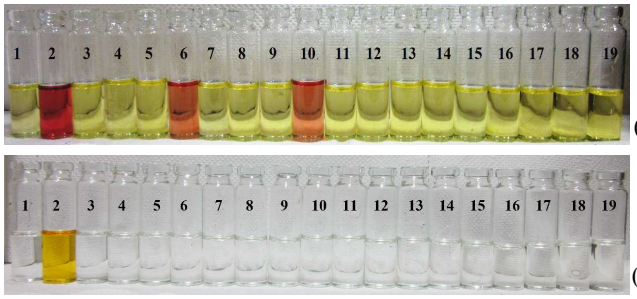

Fig. 2 Visual response of (a) **P1** and (b) **P2** with different anions; [Vial 1. **P1**/**P2** (blank), 2. F^-, 3. Cl^-, 4. Br^-, 5. I^-, 6. OAc^-, 7. SO_4^{2-}, 8.$C_2O_4^{2-}$, 9. SCN^-,10. $H_2PO_4^-$, 11. HPO_4^{2-}, 12. HSO_4^-, 13. ClO_4^-, 14. PF_6^-, 15. BF_4^-, 16. N_3^-, 17. NO_2^-, 18. NO_3^- and 19. CO_3^{2-}].

UV-Vis titration of P1 and P2 with TBA^+F^-

UV-Vis titration was carried out in room temperature with TBA salt of respective anions in order to investigate the interaction of **P1** and **P2** with different anions. In case of unbound **P1** a strong intramolecular charge transfer absorption band was found at 390nm in DMSO.[3e,8] Interaction of **P1** with TBA salt of F^- resulted in a red shift of the charge transfer (CT) band by ~100 nm (Fig. 3a). Interaction of hydrogen bond donor -NH group with guest F^- is coupled through Intermolecular proton transfer (IPT)[2] from **P1** to F^-. Proton abstraction from -NH unit produces negative charge on N atom of sensor **P1**, as a whole enhancement of intramolecular charge transfer (ICT) transition was happened due to push pull nature. In addition, presence of $-NO_2$ like chromophore led to visible colorimetric changes from yellow to red, which is detectable in naked eye (Fig. 3).[2] In reality, response at 390 nm was gradually minimized with simultaneous appearance of a new band at 490 nm. The clear isosbestic point at 430 nm suggests that only one type of host-guest (host: **P1** and guest: F^-) complex exists.[9]

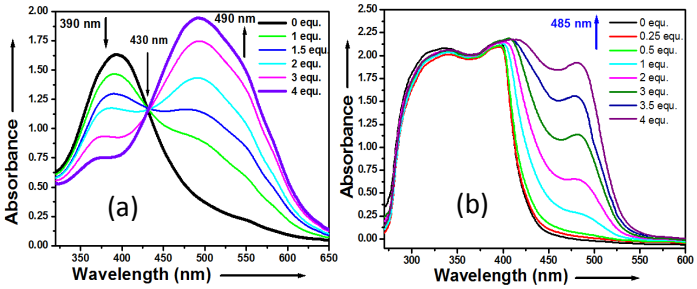

Fig. 3 UV-Vis absorption changes of (a) **P1** and (b) **P2** with gradual addition of TBA^+F^- in DMSO at room temperature.

It was cleared from color change that **P2** changes from colorless to bright yellow after interaction with F^-. There are two bands at 330nm and 395nm respectively in DMSO. The band at 330 nm can be attributed for transition between the π orbital localized on central bond of azomethine group (-CH=N-).[8] Low energy band at 395 nm can be the effect of an intramolecular charge transfer within **P2**.[2] After interaction of **P2** with F^- the second band at 395 nm was red shifted to 415 nm. Generation of the new peak at 485 nm (Fig. 3) can be assigned to Charge transfer transition between anion receiving unit (N-H···F^-) and cyano unit. Association equilibrium constant (at 298 K) of **P1** and **P2** with F^- is 6.6 x 10^3 M^{-1} and 3 x 10^3M^{-1} respectively (see ESI,† for details regarding determination method, *i.e.*; Benesi Hildebrand equation, Fig. S5). To establish **P1** and **P2** as a universal sensor, the interference study of the sensors for F^- was carried out with other tested anions (Cl^-, Br^-, I^-, SO_4^{2-}, $C_2O_4^{2-}$, SCN^-,

HPO_4^{2-}, HSO_4^-, ClO_4^-, PF_6^-, BF_4^-, N_3^-, NO_2^-, NO_3^- and CO_3^{2-}) (see Fig. S6, ESI†).

An interesting observation is noticed in the UV-Vis titration spectra for both **P1** and **P2** with F^-. When H^+ is added to the solution containing a **P1**/**P2**$\cdots F^-$ mixture, the new response at 495 nm for **P1** and 485 nm for **P2** are quenched. In case of **P1**$\cdots F^-$ mixture solution, after addition of H^+ the new peak (490 nm) is slowly diminished with gradual generation of the old peak at 390 nm. Similarly, for **P2**$\cdots F^-$ mixture the similar type of observation is found, where the new peak at 485nm is diminished with addition of H^+. The response of sensor **P1** and **P2** (*i.e.;* without fluoride) is actually unaltered with addition of same equivalent of H^+ only. Thus from chemical perspective it is clear that H^+ actually inhibits the hydrogen bonding interaction between F^- and host **P1** and **P2**, as H^+ has better affinity towards highly negative F^- in comparison with hydrogen centre of **P1** and **P2** having δ^+ charge. This kind of repeatable reversibility with alternate addition of F^- and H^+ is observed clearly for more than five cycles (Fig. 4).

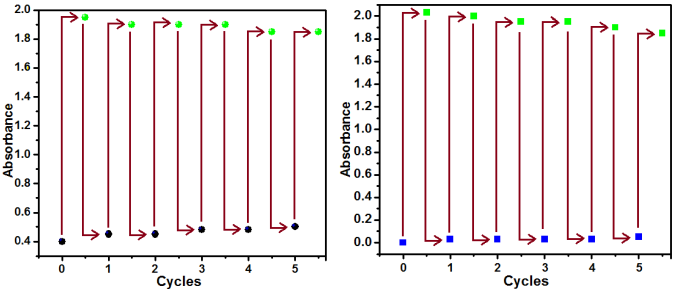

Fig. 4 Reversibility of UV-Vis response (up to five cycles) with alternate addition of F^- and H^+ for (a) **P1** (black circle: initial optical density of **P1** & green circle: final optical density of **P1** with F^-) and (b) **P2** (blue square: initial optical density of **P2** & green square: final optical density of **P2** with F^-).

Proposition for electronic circuit fabrication based on different logic gate

Table 1 Truth table for **P1** with F^- and H^+

Inputs			Outputs	
A(**P1**)	B(F^-)	C(H^+)	Y1(390nm)	Y2(490nm)
0	0	0	0	0
1	0	0	1	0
0	1	0	0	0
0	0	1	0	0
1	1	0	0	1
1	1	1	1	0
0	1	1	0	0
1	0	1	1	0

The reversible behavior of **P1** and **P2** with F^- mimics several interesting logic gate function. Sensitive responses of **P1** and **P2** towards guest F^- instigate us to fabricate Boolean logic gates and molecular level arithmetic calculation.[7]

The spectroscopic outcomes of **P1** with F^- and H^+ are tabulated in Table 1. Arithmetic calculation based on the truth table results in several logic functions, *e.g.;* AND, NOT, NOR, OR, XNOR and XOR. Altogether combination of these logic functions fabricates interesting complex circuit (Fig. 5). We have noticed that with addition of H^+ the output at 490nm minimizes and simultaneously reverted the original response of **P1** at 390nm (Y1). Incremental additions of F^- will again generate the response at 490nm (Y2). Therefore two reversible outputs are noticed; Y1 at λ_{max} 390 nm and Y2 at λ_{max} 490 nm. This generated circuit can be designated as a dual channel output mode. The inputs are A: **P1**, B: F^- and C: H^+. Output (Y1) will be ON (*i.e.*; 1) if input A is ON (*i.e.*; 1) which means blank **P1** (without F^-) shows the output at Y1. When B (*i.e.*; F^-) is ON, the output Y1 becomes OFF and simultaneously Y2 is ON; thus an implementation of AND logic function is possible here. Input C, *i.e.;* H^+ as inhibitor when ON will inhibit the hydrogen bonding interaction between **P1** and F^- : this is an implementation of inverter, *i.e.;* NOT gate. The simulation of the truth table input and output on the proposed logic circuit has been carried out successfully and summarized in supporting information, Fig. S7.

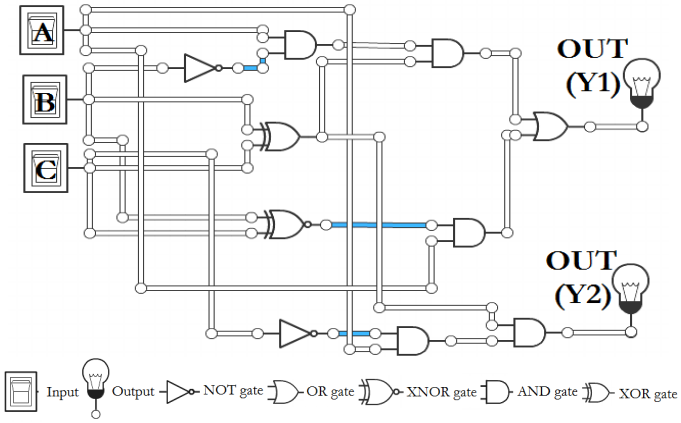

Fig. 5 Sequential combination of AND-NOT-XOR-OR-XNOR logic functions with the spectroscopic outcomes of **P1** with F^- and H^+.

Interestingly, reversible type of response by alternate addition of F^- and H^+ to the sensor **P1** solution in UV-Vis study switches a sequential logic circuit displaying "***Write-Read-Erase-Read***" sequences in line with binary logic (Fig. 6).

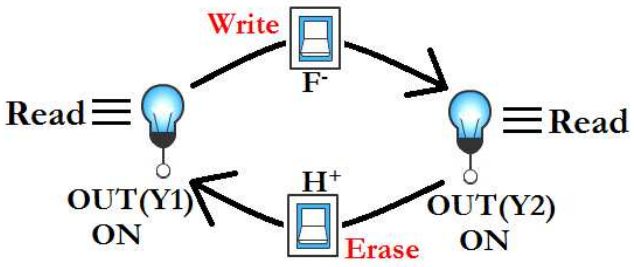

Fig. 6 Proposed loop demonstrating the reversible logic operations with '***Write–Read–Erase–Read***' function.

In electronic devices fabrication, NOR logic function is considered to be a universal logic gate. Apollo guidance computer actually uses more than 4,000 integrated circuits (ICs), each IC contains several NOR gate. Keeping in mind the applicability of NOR logic function in real practice, we have explored the possibility of development of electronic circuit based on NOR logic function. The truth table 1 successfully mimics AND-NOT-NOR-XOR-OR-XNOR logic function (Fig. S8). The simulation of the truth table input and output on the proposed logic circuit has been carried out successfully and summarized in supporting information, Fig. S8.

The spectroscopic outcomes of **P2** with F^- shows the generation of new peak at 485 nm which upon addition of H^+ minimizes as H^+ inhibits the hydrogen bonding interaction between **P2** and F^-. The outcomes are tabulated with single output (Y'= λ_{max} 485nm) in Table S4. The inputs are A': **P2**, B': F^- and C': H^+. Several combination of Boolean logic function can be obtained with proper arithmetic calculation of the outcomes in Table S4.

Initially, the outcome of UV-Vis titration study is mimicking an AND logic gate function where two chemical inputs are sensor **P2** (A') and F^- (B') respectively. Output (Y') is the new enhanced signal with higher optical density at 485nm for **P2** (A') after interacting

with F^- (B'). The output will be ON (*i.e.;* 1) if inputs are ON (*i.e.;* 1) which means if both inputs are 'ON' then only output is 'ON' otherwise 'OFF'. The results are fitted in 2 input AND logic gate function. As H^+ inhibits the hydrogen bonding interaction between **P2** and F^-, therefore use of H^+ as third chemical input (*i.e.;* C') will imply a new logic function, *i.e.;* NOT logic function (INHIBIT logic function as per truth Table S4, Fig. S9, ESI†). The successful validation of the truth table S4 on the developed circuit has been shown in Fig. S9.

Implementation of NOR as universal logic gate are very important from designing point of view of electronic devices. Thus, using the truth table (Table S4, ESI†) another logic circuit using NOR logic function has also been developed (NOT-NOR-OR gate circuit with different inputs, Fig. S10, ESI†). The validation of the truth table on the developed circuit has been successful and is shown in Fig. S10.

Another interesting logic function is XOR gate. XOR function can be used as a one bit adder, which can add any two bits together to one bit output. Pseudo random number (PRN) generators are particularly linear feedback shift registers actually defined in terms of XOR operation. All this motivate us to propose another logic circuit based on XOR function (AND-NOT-XOR-OR gate circuit with different inputs Fig. S11, ESI†). The validation of the truth table S4 on the developed circuit has been successful and shown in Fig. S11.

Fluorescence titration of P1 and P2 with TBA^+F^-

In DMSO:water (4:1,v/v, HEPES buffer, pH 7.4) the emission properties of **P1** and **P2** sensor was thoroughly investigated in presence of TBA^+F^-. **P1** ($1x10^{-5}$M) shows the response at 475 nm in DMSO:water (4:1,v/v, HEPES buffer, pH 7.4) on excitation at 390 nm wavelength. On gradual addition of TBAF (~2 equivalents) the peak at 475 nm slowly diminished and simultaneously blue shifted to 450 nm. Peak enhancement was observed after addition of 2 equivalents of F^- in emission spectrum with blue shift and a new peak was also generated at 415nm with a distinct isoemission point at 450nm (Fig. 7a). Both Intramolecular charge transfer (ICT) and Photoinduced electron transfer (PET) mechanism can be applicable to explain the outcome. The difference between PET and ICT mechanism for a sensor lies in the different fluorimetric response upon guest analyte recognition. Actually, PET probe shows enhancement or quenching in fluorescence response without distinct spectral shifts. In comparison, sensor based on ICT shows clear spectral shifts in fluorescence responses upon analyte binding.[10]

In case of **P1**, gradual addition of F^- resulted in hydrogen bond formation in initial stage. The loewdin population analysis in modern DFT study it was reflected that addition of 1 equivalent F^- resulted in an enhancement in electron density on nitrogen atom of –NH unit for **P1**(Table S6-S7, ESI†). Through-bond propagation was responsible for the enhancement of electron density on phenyl rings (counter supported by proton NMR study), which in turn responsible for photoinduced electron transfer process, eventually quenching of fluorescence was observed. Excess addition (~4 equivalents) of F^- ended up with deprotonation of the –NH proton and electron density on -NH centre nitrogen increased (also supported by DFT-D3 calculated Loewdin population analysis, Table S8-S9, ESI†). As a consequence, in **P1** extent of intramolecular charge transfer (ICT) from the deprotonated nitrogen atom to the nitro group is enhanced (Lifetime measurement by time-correlated single photon counting method for **P1** was found 4.42ns, which lowered down after addition of fluoride and became 2.12ns).[10,11a] Enhancement in ICT provides a shift in the wavelength as a function of F^- concentration and fluorescence was recovered.[11b] Hence for **P1**, the emission intensity at 475 nm is gradually '*turned off*' over incremental addition of F^- and simultaneously the emission signal at 415 nm is '*turned on*'.

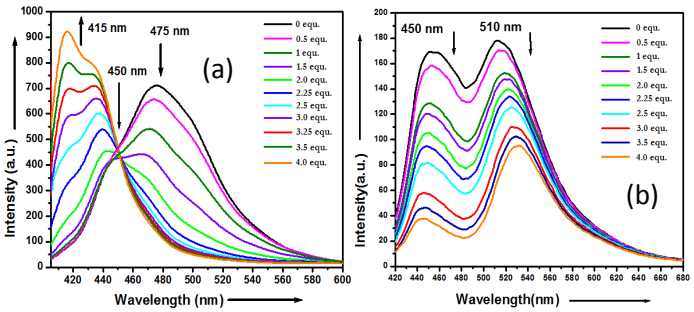

Fig. 7 Fluorescence titration spectra in DMSO:water (4:1,v/v, HEPES buffer, pH 7.4) (a) **P1** and (b) **P2** with TBA^+F^-.

In case of **P2,** incremental addition of F^- resulted in development of hydrogen bonded network within **P2**. Loewdin population analysis suggests that addition of 1 equivalent F^- resulted in an enhancement in electron density on nitrogen atom of –NH unit for **P2** (*vide* Table S10-S13, ESI†). Through-bond propagation helps in enhancement of electron density in phenyl rings. Obviously, photoinduced electron transfer (lifetime of **P2**: 0.22ns, for **P2•••**F^- complex: 1.45ns) takes place and quenching of fluorescence happened (Fig. 7b).[11b,11c]

^{1}H-NMR titration of P1 and P2 with TBA^+F^-

Plausible binding mode of **P1** and **P2** with TBA^+F^- proposed from UV-Vis and fluorescence titration study is finally validated by exploratory ^{1}H-NMR study. ^{1}H-NMR study reveals that -NH proton signal at ~11.7 ppm moves to downfield and then finally diminishes upon addition of 2equivalent F^- due to deshielding of electron through N-H···F^- hydrogen bonded complexation. Addition of 3 equivalents F^- is resulted in formation of HF_2^- at ~16.1 ppm, suggesting the deprotonation. As **P1** become electron rich therefore other protons inside the skeleton moves to upfield, facing the higher electron density (Fig. 8a). The deprotonation is occurring here mainly due to three factors: (i) presence of two -NO_2 groups make the -NH protons highly acidic; (ii) resonance stabilized species formation and (iii) formation of thermodynamically stable [HF_2^-] species leads the equilibrium to the right.

The prediction in previous section regarding the binding of **P2** with F^- is authenticated by ^{1}H-NMR study. The acidity of N-H proton in **P2** is not as much as of **P1** and ultimately not abstracted but diminished with downfield shifting due to deshielding of electron through hydrogen bonding; HF_2^- formation was not observed even after addition of more than 4 equivalents of F^-. As no proton is abstracted from **P2**, in its consequence the whole scaffold does not face any higher electron density, eventually are remained unaltered in their proton peak position (Fig. 8b).

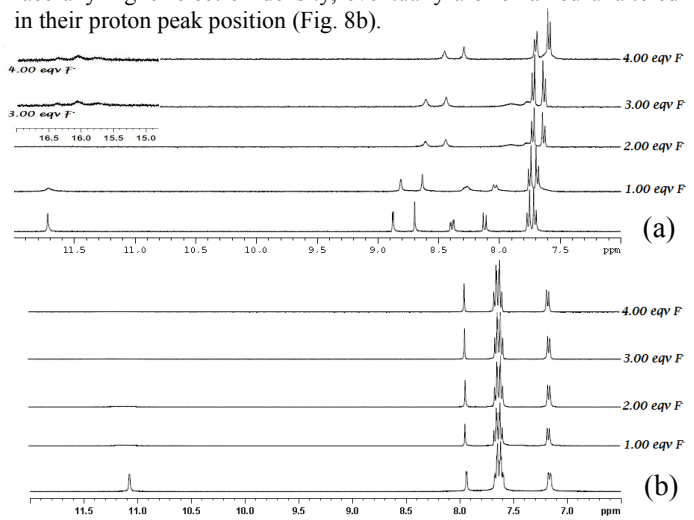

Fig. 8 ^{1}H-NMR titration spectra of (a) **P1** (inset shows HF_2^- peak at ~16.1 ppm) and (b) **P2** with TBA^+F^- in DMSO-d_6.

DFT-D3 study

Density Functional Theory is used in order to verify the host and guest complexation from a theoretical perspective. In **P1** like sensor with higher acidic proton the recognition process is based on Acid-Base mechanism. In **P2** with less acidic proton there is hydrogen bonding interaction between host and guest which is considered to belong in realm of Supramolecular Chemistry.

Our target is to correlate the experimental and theoretical outcome for both sensor **P1** and **P2** and also to establish the methodology by which it will be easy to predict the level of sensitivity and selectivity towards fluoride before doing experiments. In order to achieve insight in host-guest interaction, more specifically, to find out the sensing pathway is whether based on hydrogen bonding interaction or proton abstraction, DFT-D3 calculation has been taken into consideration.

In ^{1}H-NMR study, HF_2^- formation has been noticed for sensor **P1**, but for sensor **P2** no such peak was observed. So, to understand the detail of the complexation of sensor and sensing anions, a detail computational calculation were performed. The computational calculation performed by considering the weak interaction using ORCA (version 3.0.0, developed by Prof. Dr. Frank Neese).[12] The functional chosen here was B3LYP with the Grimme's third generation dispersion correction *i.e.*; DFT-D3. Also Becke-Johnson damping parameter was included during the calculation.

Initially we have carried out manual conformational search for sensor **P1**, and most stable geometry was determined for the study (Table S5, ESI†). In case of **P2** the coordinates and stabilized geometry was obtained from single crystal X-ray structure data sets. After geometry optimization of both **P1** (Fig. 9a, Table S6) and **P2** (Fig. 10a, Table S10), we have taken the geometries for further study of complexation with guest F^- ion (charge is counter balanced by NMe_4^+). For sake of simplicity and doing theoretical studies in lesser time we have used NMe_4F instead of NBu_4F.

In case of sensor **P1**, NMe_4F was added first to the optimized geometry of **P1**, keeping the NMe_4F at different position around **P1**. After generation of different conformers those were optimized and the most stable geometry had been considered (Fig. 9a, Table S6). In the optimized geometry of the 1:1 (**P1**: F^-) complex, the hydrogen atom (H1) bonded with N1 forms hydrogen bonded structure with guest F^- (F1) (Fig. 9b, Table S7). The atomic distance between H1 and N1 in 1:1 complex is 1.123 Å, whereas before the complexation the distance was 1.025 Å (Fig. 9a). The distance between H1 and F1 is 1.367 Å, which reflects the generation of strong hydrogen bond. Furthermore, calculation in presence of one more NMe_4F resulted in a 1:2 complexation where the geometry of the **P1** becomes out of the plane (Fig. 9c, Table S8). In 1:1 complex H1 was weakly bonded to N1 however in 1:2 complex type host guest system H1 completely removed and forms bond with F1 (H1-F1= 0.995 Å). N1-H1 interatomic distance now lies at about 1.579 Å (Fig. 9c). **P1** became electron rich as expected after detachment of H1 from the N1. In the ^{1}H-NMR, it is also observed that the peak position of the rest protons shows upfield shifting (Fig. 8a, *vide supra*). Further addition of one more equivalent of NMe_4F to the 1:2 complex, the resultant geometry of complex 1:3 did not change. In 1:3 case study, the outcomes of NMR experimentation (Fig. 8a, *vide supra*) are fully validated as the newly added F^- ion (F3) forms a bond with H1F1 (Fig. 9d, Table S9). In this consequence, generation of HF_2^- species during complexation has been observed. The bond distances of H1-F1 and H1-F3 are 1.107 Å and 1.173 Å respectively.

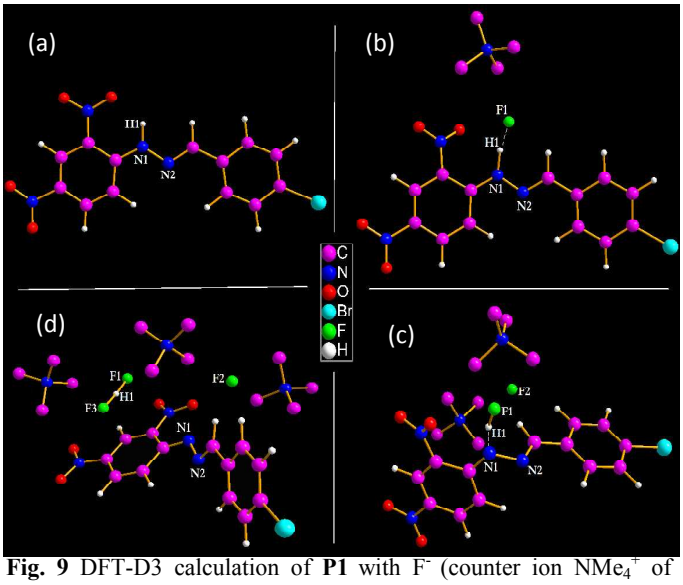

Fig. 9 DFT-D3 calculation of **P1** with F^- (counter ion NMe_4^+ of which hydrogen atoms are not shown for clarity, computational level: B3LYP-D3(BJ)/def2-SVP).

The coordinates and subsequent geometry of sensor **P2** was taken from the X-ray crystal structure and optimized (Fig. 10a, Table S10). The N1-H1 bond distance in optimized structure of **P2** was 1.025 Å. In a geometry optimized **P2** unit, one NMe_4F was added at different position around **P2** and optimized. The most stable geometry is chosen for the further study. In the 1:1 host guest complex F^- ion forms hydrogen bond with H1 (Fig. 10b, Table S11), the hydrogen bonding distance was 1.435 Å. Again in the 1:1 complex structure the N1-H1 bond distance increased from free **P2** by 0.067 Å. One more NMe_4F addition in 1:1 complex (Fig. 10c, Table S12) did not change the geometry of the 1:2 complex, rather the similar hydrogen bonded geometry of 1:1 complex is maintained. There was no indication of formation of HF. Lastly on the basis of comparative correlation studies, another NMe_4F was included in 1:2 complex to get 1:3 complex (Fig. 10d, Table S13). Here also no indication of the formation of either HF or HF_2^- is observed, supports by ^{1}H-NMR outcomes (Fig. 8b, *vide supra*).

DFT-D3 concluded that in the fluoride recognition process, **P1** abstracts the N1H1 proton, however in **P2** the proton was no way abstracted which suggest that the fluoride recognition of **P2** belongs to the realm of supramolecular chemistry.

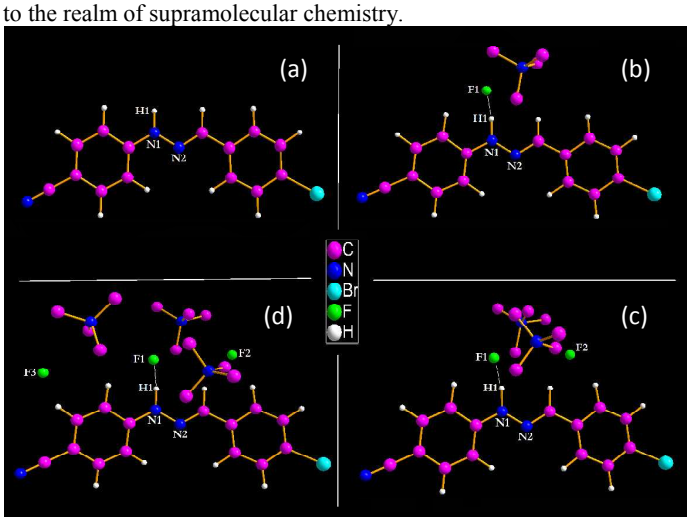

Fig. 10 DFT-D3 calculation of **P2** with F^- (counter ion NMe_4^+ of which hydrogen atoms are not shown for clarity, computational level: B3LYP-D3(BJ)/def2-SVP).

Analytical Applications

Precise modification by suitable substitution in aromatic ring has delivered a selective fluoride sensor. After visualizing the correlation between experimental and theoretical chemistry behind the engineering of a selective sensor, we are now a days interested to explore the practical utility of these sensors. In this perspective, we have explored two different domain of application:

(a) Solution kit for fluoride detection.

(b) *in vitro* F^- detection by **P1**.

(a) Solution kit for fluoride detection:

Both the sensor shows different colorimetric responses towards fluoride (*i.e.*; **P1** can sense a few selective anions by changing color from yellow to red whereas **P2** can selectively detect fluoride from colorless to bright yellow). Our emphasis is to develop a selective fluoride sensor and thus an easy to use solution kit for selective detection of fluoride from unknown samples has been fabricated.

(i) The solution kits are prepared with the DMSO solution of sensors (**P1** and **P2**) in a 10^{-4}M concentration. For **P1** the color of the kit is yellow and for **P2** it is color less (Fig. 11).

(ii) 2-3 drops (else 10-30μL) of unidentified sample in DMSO:Water (4:1) solvent mixture was poured on the test kit. It was noticed that **P1** kit has shown an instant red color towards F^-/OAc^- (strong response) or $H_2PO_4^-$ (comparatively weaker response). On the other way **P2** kit has shown colorless to bright yellow change for fluoride selectively.

(iii) In spite of development **P2** kit for specific and selective detection of F^-, we have still prepared **P1** kit in order to distinguish OAc^- and $H_2PO_4^-$ from F^-. A sample showing colorimetric response in **P1** kit, may give an idea about presence of $F^-/OAc^-/H_2PO_4^-$ in solution, if no change in color then obviously other anions are present (Cl^-, Br^-, I^-, SO_4^{2-}, $C_2O_4^{2-}$, SCN^-, HPO_4^{2-}, HSO_4^-, ClO_4^-, PF_6^-, BF_4^-, N_3^-, NO_2^-, NO_3^-, CO_3^{2-}). If that unidentified sample shows bright yellow color in **P2** kit then certainly it contains fluoride, if no response towards **P2** kit but shows color change in **P1** kit then certainly the unknown sample contains either OAc^- or $H_2PO_4^-$. Our group have previously reported sensor which can recognize OAc^- and $H_2PO_4^-$ fluorimetrically. The reported sensor shows '*turn on*' fluorescence response towards $H_2PO_4^-$ and remains unresponsive for OAc^-.[3e] Therefore solution kit for detection of fluoride selectively from an unknown sample have been developed successfully.

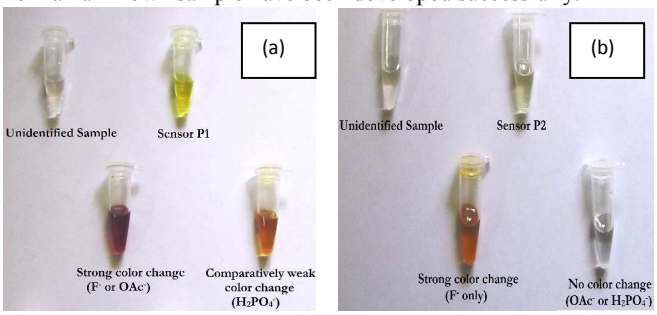

Fig. 11 Solution kit for fluoride detection (a) **P1** and (b) **P2**.

(b) *in vitro* F^- detection by P1:

In vitro detection of F^- for quick and easy identification of non skeletal fluorosis is also of prior importance as non skeletal fluorosis affects all the soft tissues and organs of human body. Interestingly, after incubation with F^- contaminated water of Bankura,[5b] West Bengal, when **P1** is added to the cells [two different types of cells *viz.* pollen grains of *Techoma stans* (Fig. 12) and *Candida albicans* (Fig. S13) were used for in vitro fluoride detection, for details, please see supporting information, ESI†] blue emission is observed which confirms the detection of intracellular F^-. The result indicates that **P1** can be used to detect the presence of intracellular F^- in samples (living cells such as bacteria, fungi, protozoa *etc*).

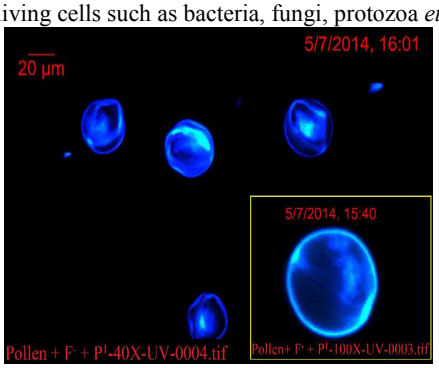

Fig. 12 *In vitro* detection of F^- in ppm level concentration by **P1** in Pollen grains (inset shows the image under 100X lens).

Conclusions

In summary, two novel neutral Schiff base chemosensors have been synthesized and characterized for fluoride ion detection, where substitution in the aromatic ring plays the key role in making a selective fluoride chemosensor. Host-guest type interaction was confirmed through UV-Vis, fluorescence and ^{1}H-NMR like sophisticated analytical tools. Interesting outcomes of UV-Vis titration mimics several logic gate operations and complex electronic circuits. Fluorescence '*turn on* and *off*' characteristics are noticed for the sensors with fluoride. DFT-D3 has been executed in order to correlate the experimental and theoretical outcome. Significantly, *in vitro* fluoride recognition under fluorescence microscope is successful in ppm level and it is believed that this methodology might be useful for further research in bio-medical appliance. Furthermore, an easy to use solution test kit for tracing F^- from DMSO:Water (4:1) aqueous solvent mixture is also developed. Our research on development of several small organic sensor molecules with colorimetric sensing ability for various bio essential anions is now under active progress.

Acknowledgement CSIR-Supra institutional research fund under CSIR-XIIth five year plan (Govt. of INDIA) is gratefully acknowledged (ESC-0203/9). Department of Science and Technology, Govt. of INDIA sponsored Fast Track Project (*vide* ref. no: SB/FT/CS-003/2012 and project no: GAP-183112) for a young researcher is also acknowledged for carrying out the computational work. PG is thankful to Department of Science and Technology, Govt. of INDIA (GAP-183112) for his fellowship. Thanks are due to Dr. Anakuthil Anoop for many helpful discussions. Authors are extremely thankful to Dr. N. C. Murmu, Surface Engineering & Tribology Group for constant support and encouragement.

Notes and references

[a] *Surface Engineering & Tribology Group, CSIR-Central Mechanical Engineering Research Institute, Mahatma Gandhi Avenue, Durgapur-713209, District: Burdwan, West Bengal India.*
E-mail: pr_banerjee@cmeri.res.in & priyabrata_banerjee@yahoo.co.in
Webpage: www.cmeri.res.in & www.priyabratabanerjee.in
Fax: +91-343-2546745; Tel: +91-343-6452220.
[b] *Academy of Scientific and Innovative Research at CSIR-CMERI, Durgapur 713209, India.*
[c] *Department of Chemistry, Sikkim University, Gangtok-737102, Sikkim, India.*
[d] *Department of Chemistry, Indian Institute of Technology Kharagpur, Kharagpur, West Bengal, India - 721 302.*
[e] *Department of Microbiology, The University of Burdwan, Burdwan 713104, India.*

†Electronic Supplementary Information (ESI) available: [Experimental details of **P1** and **P2** preparation. Crystallographic details of **P2**, ESI-MS

and ^{1}H-NMR of **P1** and **P2** are provided. DFT calculation details, coordinates used for **P1** and **P2** has been provided. Details regarding cell images are accounted. Crystallographic information of **P2** reported in this article is available in the Cambridge Crystallographic Data Centre as deposition No. CCDC: 1043089]. See DOI: 10.1039/b000000x/

1 (a) T. Gunnlaugsson, M. Glynn, G. M. Tocci, P. E. Kruger and F. M. Pfeffer, *Coord. Chem. Rev.*, 2006, **250**, 3094; (b) P. A. Gale, *Coord. Chem. Rev.*, 2003, **240**, 191.

2 M. A. Kaloo and J. Sankar, *Analyst*, 2013, **138**, 4760 and references there in.

3 (a) P. Ghosh, S. K. Saha, A. Roychowdhury and P. Banerjee, *Eur. J. Inorg. Chem.*, 2015, 2851; (b) P. Ghosh, B. G. Roy, S. K. Mukhopadhyay and P. Banerjee *RSC Adv.*, 2015, **5**, 27387; (c) P. Ghosh, A. R. Chowdhury, S. K. Saha, M. Ghosh, M. Pal, N. C. Murmu and P. Banerjee, *Inorg. Chim. Acta*, 2015, **429**, 99; (d) P. Ghosh, A. Roychowdhury, M. Corbella, A. Bhaumik, P. Mitra, S. M. Mobin, A. Mukherjee, S. Basu and P. Banerjee, *Dalton Trans.*, 2014, **43**, 13500; (e) A. Roychowdhury, P. Ghosh, S. K. Saha, P. Mitra and P. Banerjee, *Spectrochim. Acta. Part A,* 2014, **124**, 492; (f) P. Banerjee, A. D. Jana, G. Mostafa and S. Goswami, *Eur. J. Inorg. Chem.,* 2008, 44; (g) P. Banerjee, S. Kar, A. Bhaumik, G-H. Lee, S-M. Peng and S. Goswami, *Eur. J. Inorg. Chem.,* 2007, 835; (h) S. Das, P. Banerjee, S-M. Peng, G-H. Lee, J. Kim and S. Goswami, *Inorg. Chem.*, 2006, **45**, 562; (i) A. R. Chowdhury, P. Ghosh, B. G. Roy, S. K. Mukhopadhyay, N. C. Murmu, P. Banerjee, *Sens. Actuators, B*, 2015, **220**, 347.

4 (a) I.-S. Ke, M. Myahkostupov, F. N. Castellano and F. P. Gabbaï, *J. Am. Chem. Soc.*, 2012, **134**, 15309; (b) H. Miyaji, W. Sato and J. L. Sessler, *Angew. Chem., Int. Ed.*, 2000, **39**, 1777.

5 (a) K. Youngmin and F. P. Gabbaï, *J. Am. Chem. Soc.*, 2009, **131**, 3363; (b) S. Jagtap, M. K. Yenkie, N. Labhsetwar and S. Rayalu, *Chem.Rev.*, 2012, **112**, 2454.

6 (a) T. Nishimura, Su-Y. Xu, Y-B. Jiang, J. S. Fossey, K. Sakurai, S. D. Bull and T. D. James, *Chem. Commun.*, 2013, **49**, 478; (b) Y. Zhou, J. F. Zhang and J. Yoon, *Chem. Rev.*, 2014, **114**, 5511.

7 (a) B. L. Feringa, Molecular Switches, Wiley-VCH Express, New York, 2001, p. 37; (b) J. Millman and A. Grabel, Microelectronics, McGraw-Hill, New York, 1988, ch. 6; (c) K. Rezaeian and H. Khanmohammadi, *New J. Chem.,* 2015, **39**, 2081; (d) J. Andréasson and U. Pischel, *Chem. Soc. Rev.*, 2015, **44**, 1053; (e) S. Sreejith and A. Ajayaghosh, *Indian J. Chem.*, 2012, **51**, 47; (f) J. Ling, B. Daly, V. A. D. Silverson and A. P. de Silva, *Chem. Commun.*, 2015, **51**, 8403; (g) A. P. de Silva, I. M. Dixon, H. Q. N. Gunaratne, T. Gunnlaugsson, P. R. S. Maxwell and T. E. Rice, *J. Am. Chem. Soc.*, 1999, **121**, 1393.

8 H. H. Hammud, A. Ghannoum, M. S. Masoud, *Spectrochim. Acta Part A*, 2006, **63**, 255.

9 V. Kumar, M. P. Kaushik, A. K. Srivastava, A. Pratap, V. Thiruvenkatam and T. N. Gururow, *Anal. Chim. Acta*, 2010, **663**, 77.

10 N. Boens, V. Leen and W. Dehaen, *Chem. Soc. Rev.*, 2012, **41**, 1130.

11 (a) N. B. Sankaran, P. K. Mandal, B. Bhattacharya and A. Samanta, *J. Mater. Chem.*, 2005, **15**, 2854; (b) A. K. Mahapatra, P. Karmakar, J. Roy, S. Manna, K. Maiti, P. Sahoo and D. Mandal, *RSC Adv.*, 2015, **5**, 37935; (c) E. Arunkumar and A. Ajayaghosh, *Chem. Commun.*, 2005, 599.

12 ORCA 3.0.0, developed by Prof. Dr. Frank Neese, Max Planck Institute for Bioinorganic Chemistry, Muelheim/Ruhr, Germany.